

Investigating the Relationship between Pneumatized Middle Turbinate and Anterior Ethmoid Roof Dimensions Using CBCT Images

Arezoo Mirshekari ¹, Abdolaziz Haghnegahdar ², Seyed Ghasem Mirbaba ³,
Sarina Hassanpour Dargah ^{3*}

1. Department of Pediatric Dentistry, School of Medical Science, Kerman University of Medical Sciences, Kerman, Iran
2. Department of Oral and Maxillofacial Radiology, School of Medical Science, Shiraz University of Medical Sciences, Shiraz, Iran
3. Department of Oral and Maxillofacial Surgery, School of Medical Science, Kerman University of Medical Sciences, Kerman, Iran

ABSTRACT

Background: Understanding the anatomical relationship between the pneumatized middle turbinate (PMT) and ethmoid roof structures is crucial for minimizing complications in endoscopic sinus surgery. We aimed to evaluate the association between PMT and the dimensions of the anterior ethmoid roof using cone-beam computed tomography (CBCT) imaging.

Methods: A retrospective, cross-sectional study was conducted on 249 CBCT scans obtained at a maxillofacial radiology center. All images were acquired using a NewTom VGi scanner (QRsrl, Verona, Italy) with a 15×15 cm field of view and 1-mm slice thickness. Measurements were taken from coronal sections displaying the infraorbital nerve canal. Key anatomical points, including the medial and lateral ethmoid roof points (MERP and LERP) and the cribriform plate (CP), were identified. The width and height of these structures were measured. PMT was classified as lamellar, bulbous, or extensive. Statistical analyses included chi-square, t-test, and Pearson correlation tests.

Results: A significant relationship was found between the axial dimensions of PMT and the anterior ethmoid roof width (AER) in both genders ($P < 0.05$). Differences in ethmoid roof dimensions were statistically significant between PMT types. In males, vertical PMT dimensions were correlated with CP and AER height. AER width was greater in males than females, particularly in cases with PMT.

Conclusion: A close anatomical relationship exists between PMT and ethmoid roof dimensions, especially AER width. Recognition of these variations is essential for surgical planning and avoiding complications in sinus and skull base surgery.

*Corresponding Author:

Sarina Hassanpour Dargah

Department of Oral and Maxillofacial Surgery, School of Medical Science, Kerman University of Medical Sciences, Kerman, Iran.

Email:

sarina.hassanpour@gmail.com

Received: ***

Accepted: ***

KEYWORDS

Anterior ethmoid roof; Cone Beam Computed Tomography; Pneumatized Middle turbinate

Please cite this paper as:

Mirshekari A, Haghnegahdar A, Mirbaba SG, Hassanpour Dargah. Investigating the Relationship between Pneumatized Middle Turbinate and Anterior Ethmoid Roof Dimensions Using CBCT Images. *World J Plast Surg.* 2025;14(4):1-11.
doi: 10.61186/wjps.14.4.**

INTRODUCTION

The ethmoid sinus develops during the fifth and sixth months of the embryonic period by advancing the nasal epithelium into its lateral cartilaginous wall. The increase in size of the air cells is limited by the adjacent cells and the presence of bone, and ultimately, a structure resembling a beehive is created due to the thin bony septa separating them. The ethmoid air chamber is seen as a quadrangular or trapezoidal shape in the axial view¹⁻³. This chamber is divided internally by the Ethmoidal lamella or basal lamella into two anterior and posterior parts, with the anterior and posterior air cells draining into the middle and superior mesenteric sinuses⁶⁻⁴. The medial part of the ethmoid bone forms the middle turbinate. Like other adjacent bones, this turbinate may be pneumatised by the ethmoid sinus, an anatomical variation called the concha bullosa of the middle turbinate or pneumatised middle turbinate. There is a close relationship between the development of the middle turbinate and the ethmoid bone, which makes it likely that the formation of the roof of the ethmoid sinus is affected by the pneumatisation of the middle turbinate^{1,7}. Middle nasal turbinate is a crucial anatomical component because it is the most important reference during endoscopic interventions on the paranasal sinuses and a structure that affects the middle nasal passage aerodynamics^{8,9}. To prevent and reduce complications, especially major complications like cerebrospinal fluid leak, damage to the ocular nerve, damage to intracranial vessels, meningitis, hemorrhage, infection, adhesions, constriction or narrowing of the osteoma, , and increase the chance of surgical success, the surgeon should be aware of the anatomical variations in the skull base and its affinities such as the roof of the ethmoid, the olfactory fossa, the Lateral Lamella (LL), and the course of the anterior ethmoid artery. The fovea ethmoidalis (FE) is a normal extension of the orbital plate of the frontal bone that forms the roof of the ethmoid air chamber and separates itself and the air cells of the ethmoid sinus from the anterior cranial fossa. The FE is connected medially to LL of the cribriform palate (CP) of the ethmoid bone, which, due to its thinness, is at high risk of injury during endoscopic sinus surgery at the skull base^{10,11}.

Given the high prevalence of concha bullosa,

several articles have investigated the relationship and influence of this anatomical variation on other anatomical variations of the paranasal sinuses^{12,13}. Gun and colleagues investigated the relationship between the concha bullosa and the dimensions of the anterior part of the ethmoid roof using a CT scan. They stated a close relationship existed between the axial dimensions of the concha bullosa and the width of the anterior ethmoid roof on both the left and right sides. Still, no significant relationship was observed between the vertical and sagittal dimensions of the concha bullosa and the width of the anterior ethmoid roof¹⁴.

In this study, the relationship between pneumatised middle turbinate and anterior ethmoid roof dimensions was investigated using cone beam computed tomography (CBCT) Imaging to give surgeons a better concept of anatomical variations and help them minimise their complications during minimally invasive procedures like Endoscopic sinus surgery.

MATERIALS AND METHODS

This cross-sectional, retrograde study was conducted on 249 CBCT images of patients referred to a maxillofacial radiology center at Shiraz University of Medical Science, Iran, during 12 months from November 2023 to October 2024. This study was approved by the ethical committee of Shiraz Medical Science University (IR.SUMS.REC.1396.S329).

All images used were obtained by a Newtom VGI device with a field of view (FOV) of 12×15 cm and a pixel size of 0.3 mm (standard model) and were viewed on a monitor at the NNT station under appropriate conditions. Of all the images obtained, only 249 images of patients were included in the study, as the other images were excluded from the study based on the Exclusion criteria, including the patients with sinonasal tumors and nasal polyps, Patients under 18 years of age, patients with Significant asymmetry in the facial skeleton and Severe inflammation that prevents visualisation of the skull base.

Image study and data extraction were performed under the direct supervision of an oral and maxillofacial radiologist. Three radiographical points were identified as references on the skull base in coronal sections, including: Lateral Ethmoid Roof Point (LERP): The intersection of the vertical tangent

line on the medial wall of the orbit with the ethmoid roof, Medial Ethmoid Roof Point (MERP): The junction of the horizontal or sloped portion of the lower part of the skull base with the lamina lateralis of the CP bone and the Cribiform Plate (Figure 1). The reference points were identified in the first coronal cut of CBCT where the infraorbital nerve is visible, and their measurement is performed using the digital ruler available in the relevant software, which eliminates the magnification effect. Additionally, by drawing a horizontal line on the hard palate in the same view, the distance between the nasal floor and the MERP, LERP, and CP locations was measured and referred to as LERP Height, MERP Height, and CP Height.

The distance between MERP and LERP was regarded as AER, while the distance between MERP and the crista galli was identified as CP width.

These points and measurements were recorded for all subjects included in the study. However, because the dimensions of the ethmoid were recorded on both the left and right sides, as well as the

dimensions of the concha bullosa, which could be unilateral or bilateral, all subjects were considered as two samples. Additionally, the presence or absence of concha bullosa in the middle turbinate splits the subjects into two groups: those with and without concha bullosa, which facilitated the comparison of the effect of concha bullosa on the aforementioned measurements.

To investigate the three-dimensional pneumatisation of the middle turbinate (PMT), the largest diameter of the concha bullosa in the three axial dimensions—vertical, sagittal, and axial—was considered and recorded as PMT-Axial, PMT-Vertical (Figure 2), and PMT-Sagittal (Figure 3).

In addition, based on the classification of Bolger et al., pneumatisation was categorized into three groups: bulbous (Figure 4), lamellar (Figure 5), and extensive (Figure 6)⁸. Then, statistical tests analyzed the effect of the presence of concha bullosa and its extent on the dimensions obtained in the three axial, vertical, and coronal views regarding the dimensions and shape of the ethmoid roof.

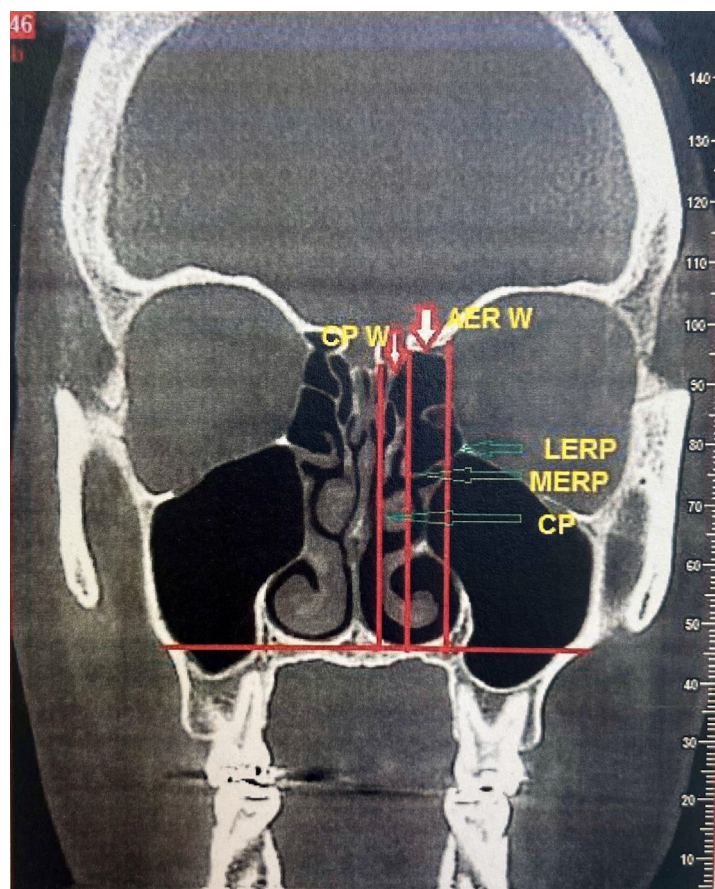


Figure 1. The width of cribriform plate (CP) and the width of anterior ethmoidal roof (AER) width and the medial and lateral ethmoid roof points (MERP and LERP)

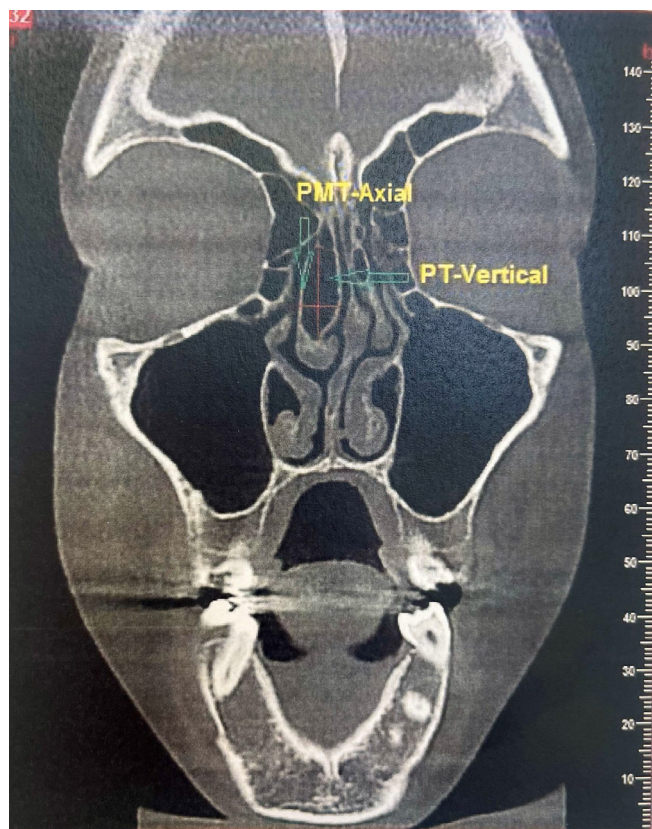


Figure 2. The axial and vertical dimensions of PMT

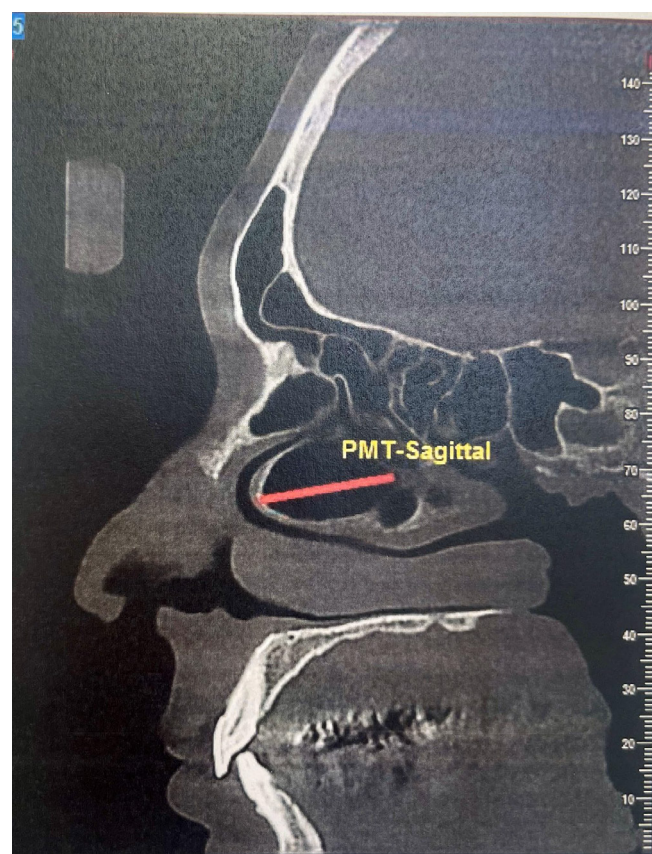


Figure 3. The sagittal dimension of PMT

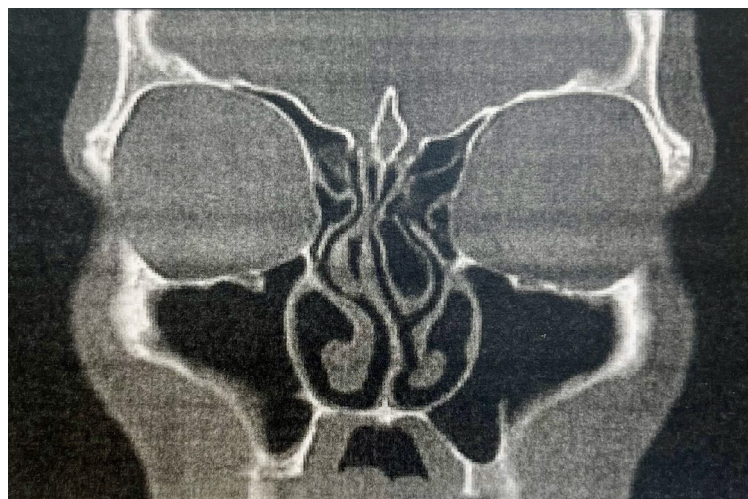


Figure 4. Bulbous type of PMT



Figure 5. Lamellar type of PMT

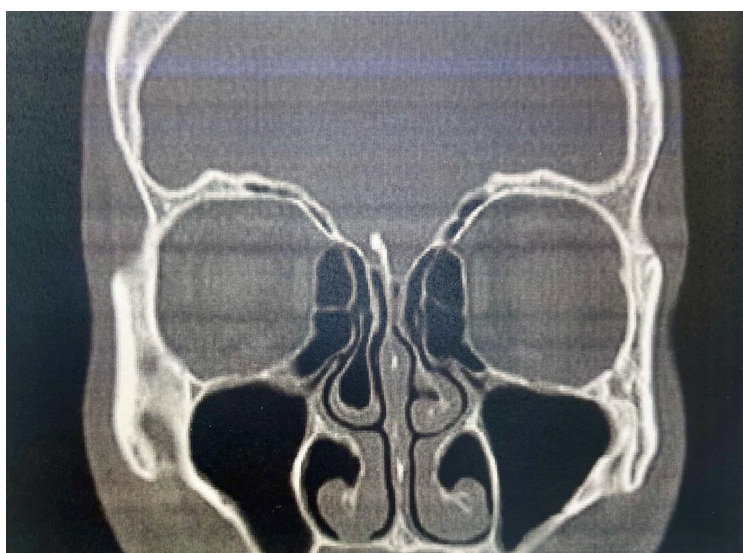


Figure 6. Extensive type of PMT

Thus, the following variables were recorded and statistically analysed: PMT in women, PMT in men, Lamellar PMT type in men and women, Bulbous PMT type in men and women, Extensive PMT type in men and women, PMT-axial diameter in men and women, PMT-vertical diameter in men and women, PMT-sagittal diameter in men and women, LERP height dimensions in men and women, MERP height dimensions in men and women, CP height dimensions in men and women, AER width dimensions in men and women, CP width dimensions in men and women.

After data collection, the study data were analyzed using SPSS version 16 software (Chicago, IL, USA). According to the statistical consultant, the comparison of the desired variables between the two groups with and without concha bullosa was performed using the student *t*-test, Chi-square test, and Paired *t*-test statistical tests, and a significance level of less than 0.05 was considered.

RESULTS

This cross-sectional study involved 249 patients undergoing paranasal CBCT imaging at a maxillofacial radiology center at Shiraz University of Medical Sciences. The subjects included 104 males and 145 females, with ages ranging from 18 to 70 years and a mean age of 31.16 years.

Out of 249 patients, 165 had concha bullosa (either unilateral or bilateral), while 84 did not have concha bullosa. Among the 165 patients with concha bullosa, 69 had unilateral concha bullosa (including 37 on the right side and 32 on the left side), and 96 had bilateral concha bullosa. In the group with concha bullosa, 53.5% were male, and 68.3% were female.

Considering that the dimensions of the ethmoid were recorded on both the left and right sides, the dimensions of the concha bullosa, which may be unilateral or bilateral, were also recorded on both sides. Each individual included in the study was treated as two samples. As a result, according to

the above, there were 498 samples in this study, of which 261 had concha bullosa (including 106 cases in men and 155 cases in women), while 237 samples included 102 cases without concha bullosa in men and 135 cases without concha bullosa in women. After examining the potential relationship between individuals with concha bullosa and those without it across all measured dimensions of the ethmoid, the following observations were noted:

The average AER width in the concha bullosa group was 8.0459 mm, whereas in the group without it, it measured 7.6669 mm ($P=0.007$) (Table 1).

The mean AER width in men with concha bullosa was 8.4237 mm, whereas in men without it, it was 7.9041 mm ($P=0.014$). Studies examining this relationship in women with and without concha bullosa revealed no significant correlation ($P>0.05$) (Table 2).

After examining the relationship between ethmoid dimensions and concha bullosa dimensions in men and women, the following results were obtained (Table 3):

In males, a significant relationship was observed between AER width and PMT-axial ($r=0.302$, $P=0.002$). Additionally, a significant relationship occurred between PMT-vertical and CP height ($r=0.195$, $P=0.046$), as well as between PMT-vertical and AER width ($r=0.241$, $P=0.011$), and again between PMT-vertical and AER width ($r=0.225$, $P=0.021$).

In females, there was a significant relationship between PMT-axial and AER width ($r=0.206$, $P=0.010$), a significant relationship between PMT-vertical and MERP height ($r=0.166$, $P=0.039$), and a significant relationship between PMT-vertical and CP height ($r=0.194$, $P=0.015$).

The prevalence of concha bullosa types based on the Bolger classification included 31 cases of bulbous concha bullosa (15 male and 16 female), 132 cases of lamellar concha bullosa (46 male and 86 female), and 98 cases of extensive concha bullosa (42 male and 56 female).

In each type of concha bullosa, the relationship

Table 1. Investigating the significance of ethmoid dimension in cases with and without concha bullosa

Variable	Mean LERP height	Mean MERP height	Mean CP height	Mean AER width	Mean CP width
With PMT	56.2912	51.2038	48.2375	8.0459	1.7283
Without PMT	56.7561	51.4772	48.5764	7.6669	1.7345
Sig(P)	$P=0.312$	$P=0.440$	$P=0.328$	$P=0.007$	$P=0.946$

between the dimensions of the concha bullosa in coronal and sagittal views and the dimensions of the ethmoid was examined. The following observations were made: In the lamellar type of concha bullosa, a significant relationship existed between PMT-axial and AER width ($P=0.010$, $r=0.233$) (Table 4).

In the bulbous type of concha bullosa, a significant relationship was identified between PMT-axial and AER width ($P=0.029$, $r=0.392$) (Table 5). No significant relationship was observed between the dimensions of the ethmoid and those of the extensive type of concha bullosa ($P>0.05$) (Table 6).

Table 2. Investigating the significance of ethmoid dimension and concha bullosa dimension in cases with and without concha bullosa based on gender

Variable	Mean LERP height	Mean NERP height	Mean CP height	Mean AER width	Mean CP width	Mean PMT-axial	Mean PMT-vertical	Mean PMT-sagittal
Men with PMT	58.2302	53.2934	50.3575	8.4237	1.7754	4.8681	12.5033	12.8574
Men without PMT	59.3480	53.7873	50.8059	7.9041	1.7519			
Women with PMT	54.9652	49.7748	46.7877	7.7875	1.6961	5.0307	12.4830	13.2839
Women without PMT	54.7978	49.7319	46.8919	7.4876	1.7214			
Sig for men(P)	$P=0.163$	$P=0.345$	$P=0.385$	$P=0.014$	$P=0.880$			
Sig for women(P)	$P=0.713$	$P=0.911$	$P=0.779$	$P=0.102$	$P=0.823$			
Sif for PMT						$P=0.620$	$P=0.976$	$P=0.568$

Table 3. Investigating the relationship between ethmoid dimension and concha bullosa dimension by gender

Variable	Sig PMT-axial	Correlation PMT-axial	Sig PMT-vertical	Correlation PMT-vertical	Sig PMT-sagittal	Correlation PMT-sagittal
Men: LERP height	$P=0.124$	0.151	$P=0.172$	0.134	$P=0.662$	0.043
Men: MERP height	$P=0.079$	0.172	$P=0.051$	0.191	$P=0.996$	0.000
Men: CP height	$P=0.138$	0.146	$P=0.046$	0.195	$P=0.826$	-0.022
Men: AER width	$P=0.002$	0.302	$P=0.011$	0.247	$P=0.021$	0.225
Men: CP width	$P=0.059$	-0.185	$P=0.936$	0.008	$P=0.296$	0.102
Women: LERP height	$P=0.243$	0.094	$P=0.240$	0.095	$P=0.192$	0.105
Women: MERP height	$P=0.532$	0.051	$P=0.039$	0.166	$P=0.102$	0.132
Women: CP height	$P=0.596$	0.043	$P=0.015$	0.194	$P=0.139$	0.119
Women: AER width	$P=0.010$	0.206	$P=0.737$	0.027	$P=0.548$	0.049
Women: CP width	$P=0.699$	0.031	$P=0.841$	0.016	$P=0.975$	-0.002

Table 4. The relationship between ethmoid dimension and the lamellar type of the concha bullosa

Variable	Sig PMT-axial(P)	Pearson correlation PMT-axial	Sig PMT-vertical	Pearson correlation PMT-vertical	Sig PMT-sagittal	Pearson correlation PMT-sagittal
LERP height	0.674	-0.037	0.964	-0.004	0.418	-0.004
MERP height	0.800	-0.022	0.425	0.070	0.409	0.073
CP height	0.407	-0.073	0.448	0.067	0.854	0.016
AER width	0.010	0.223	0.769	0.026	0.223	0.107
CP width	0.276	-0.095	0.320	-0.087	0.320	0.095

Table 5. The relationship between ethmoid dimension and the bulbous type of the concha bullosa

Variable	Sig PMT-axial(<i>P</i>)	Pearson correlation PMT-axial	Sig PMT-vertical	Pearson correlation PMT-vertical	Sig PMT-sagittal	Pearson correlation PMT-sagittal
LERP height	0.479	0.132	0.429	0.147	0.478	-0.132
MERP height	0.343	0.176	0.298	0.193	0.275	-0.202
CP height	0.279	0.201	0.161	0.258	0.233	-0.221
AER width	0.029	0.392	0.112	0.291	0.331	0.181
CP width	0.885	-0.027	0.639	0.088	0.332	-0.180

Table 6. The relationship between ethmoid dimension and the extensive type of the concha bullosa

Variable	Sig PMT-axial(<i>P</i>)	Pearson correlation PMT-axial	Sig PMT-vertical	Pearson correlation PMT-vertical	Sig PMT-sagittal	Pearson correlation PMT-sagittal
LERP height	0.328	0.100	0.620	0.051	0.127	0.155
MERP height	0.878	0.016	0.292	0.108	0.937	0.008
CP height	0.620	0.051	0.158	0.144	0.607	0.053
AER width	0.075	0.182	0.235	0.122	0.575	0.057
CP width	0.317	-0.103	0.991	0.001	0.988	0.002

DISCUSSION

The middle turbinate is usually a flat bone. However, it can be pneumatized by air cells in the anterior or, less commonly, the posterior ethmoid sinus, resulting in a common anatomical variation of the sinus known as the concha bullosa or pneumatized middle turbinate¹⁵⁻¹⁷.

Many studies have investigated the most common variation of the middle turbinate, known as concha bullosa. The prevalence of concha bullosa has been reported in various articles, ranging from 14% to 80% in adults^{11,18,19}. In one study, Stalman et al. noted a prevalence of 44%¹², while the present study recorded a prevalence of 66.3%. In contrast to Stalman's findings, the current study observed a higher prevalence of bilateral concha bullosa; among the subjects, 38.8% had bilateral concha bullosa, and only 27.7% had unilateral concha bullosa.

Former studies proposed a classification based on the location of pneumatization of the turbinates, dividing them into extensive type, bulbous type, and lamellar type^{26,27}. To date, several studies have reported the prevalence of different types of concha bullosa in adults according to this classification^{11,20-22}. In this study, the prevalence of lamellar type concha bullosa was measured at 50.6%, the prevalence of bulbous type at 11.9%, and the prevalence of

extensive type at 14.3–34%.

The prevalence of concha bullosa and its various types has been widely discussed, with several articles presenting differing results regarding its occurrence on the left and right sides. Some studies indicate a higher prevalence of concha bullosa on the left, while others report a greater prevalence on the right^{14,19,23}. This study observed that the prevalence of concha bullosa on the right side is higher than on the left.

Due to the close relationship between the middle turbinate and the ethmoid bone, it is accepted that this turbinate is part of the ethmoid bone. Conversely, the most common anatomical variation of the middle turbinate, the concha bullosa, is filled with air cells from the ethmoid sinus, which is also a component of the ethmoid bone. This variation may influence the size of the ethmoid bone, which forms part of the anterior cranial fossa. This potential effect is significant in endoscopic sinus surgeries and the unwanted complications that may arise from them^{7,25,26}.

In a study conducted by Gun et al.²⁷, the relationship between concha bullosa and the dimensions of the anterior part of the ethmoid roof was investigated. This study involved 101 patients with unilateral and bilateral concha bullosa, including 45 men and 56 women, using CT scan imaging. They also

reported that among the sides with concha bullosa, there were 67 lamellar sides, 34 bulbous sides, and 61 extensive sides. They concluded that there was a close relationship between the axial dimensions of concha bullosa and the width of the anterior ethmoid roof on both the left and right sides, with the relationship being stronger and more significant on the right side²⁷.

In comparison to the study by Gun et al.²⁷, this study examined images of the paranasal sinuses of 249 patients using the new CBCT imaging method. Of these patients, 165 had concha bullosa while 84 did not. Among the 165 patients with concha bullosa, 69 had unilateral concha bullosa and 96 had bilateral concha bullosa. Unlike the Gun study, which included only patients with unilateral or bilateral concha bullosa, this study included 84 subjects without concha bullosa. Therefore, we compared the mean AER width between the two groups, with and without concha bullosa, and found that the width of the anterior ethmoid roof was significantly greater on the side with concha bullosa.

Upon examination by gender, we observed that the mean AER width was significantly larger in men with concha bullosa. In contrast with the results of Gun et al.²⁷, Acikalin et al.²⁶ and Roman et al.²⁹, found a significant relationship between PMT-axial and AER width in men. This relationship was also reported to be significant in women^{26,27,29}.

Unlike former studies, which reported a significant relationship only between the dimensions of the concha bullosa and the width of the ethmoid roof^{27,30,31}, our study found another significant relationship between the height of the ethmoid and the dimensions of the concha bullosa, in addition to this one.

In men, a significant relationship was observed between the PMT-vertical and the height of the CP, and this relationship was also confirmed in women. Additionally, a significant relationship was noted between the PMT-vertical and the height of the MERP. Contrary to the study of Gun et al.²⁷, we examined and observed the relationship between the dimensions of the concha bullosa in both coronal and sagittal views with the dimensions of the ethmoid in each type of concha bullosa. In the lamellar type of concha bullosa, there was a significant relationship between the AER width and the PMT-axial. In bulbous type concha bullosa, there was a significant

relationship between AER width and PMT-axial. No other significant relationship was observed between ethmoid dimensions and concha bullosa dimensions in the extensive type.

CONCLUSION

After comparing and examining the side with concha bullosa to the side without it, it was observed that the width of the anterior ethmoid roof was significantly greater on the side where this anatomical variation was measured.

When we examined this case by gender, the average width of the anterior ethmoid roof (AER width) was greater in men with the concha bullosa than in men without it.

After examining the dimensions of the concha bullosa in both coronal and sagittal views, the possible relationship between the dimensions of the ethmoid bone and the sagittal, vertical, and axial dimensions of the concha bullosa was analyzed. There was a significant relationship between the axial dimensions of the concha bullosa and the width of the anterior ethmoid roof in both men and women. Additionally, in both sexes, a significant relationship was noted between the vertical dimensions of the concha bullosa and the height of the CP. Another significant relationship was reported between the vertical dimensions of the concha bullosa and the height of the MERP in women.

When we examined the relationship between the dimensions of the concha bullosa and the ethmoid by different types of concha bullosa, it was observed that in the two lamellar and bulbous types of concha bullosa, there was a significant relationship between the width of the anterior roof of the ethmoid and the axial dimensions of the concha bullosa.

ACKNOWLEDGMENTS

The authors appreciate the continued support of the Research Council of Kerman University of Medical Sciences and Student Research Committee, Kerman, Iran.

CONFLICT OF INTEREST

The authors declare that there is no conflict of interests.

REFERENCES

1. Sirikçi A, Bayazit YA, Bayram M, Ozer E, Kanlikama M. Ethmomaxillary sinus: a particular anatomic variation of the paranasal sinuses. *Eur Radiol* 2004; **14**:281–5.
2. Lee S, Choi H, Cho HJ, Kim DY. Pediatric paranasal sinuses—development, growth, pathology, and functional endoscopic sinus surgery. *Clin Anat* 2022; **35**:745–61.
3. Arredondo de Arreola G, Arredondo-Garcia JL, Ortega A. Morphogenesis of the lateral nasal wall from 6 to 36 weeks. *Otolaryngol Head Neck Surg* 1996; **114**:54–60.
4. Derin S, Sahan M, Baykal B, Tekdogan UY. Giant concha bullosa. *BMJ Case Rep* 2014; **2014**:bcr2013200524.
5. Alsaeid A. Paranasal Sinus Anatomy: What the Surgeon Needs to Know. Springer; 2017.
6. Swain SK. Middle turbinate concha bullosa and its relationship with chronic sinusitis: a review. *Int J Otorhinolaryngol Head Neck Surg* 2021; **7**:1062–7.
7. Klimenko KE, Gurov AV, Ermoshchenkova MV, Volkova AA. [Pneumatization of the middle turbinate and chronic sinusitis: current state of the problem and review of surgical correction]. *Vestn Otorinolaringol* 2025; **90**:69–74.
8. Dayal A, Rhee JS, Garcia GJ. Impact of middle versus inferior total turbinectomy on nasal aerodynamics. *Otolaryngol Head Neck Surg* 2016; **155**:518–25.
9. Kaplanoglu H, Kaplanoglu V, Bilgin G. An analysis of the anatomic variations of the paranasal sinuses and ethmoid roof using computed tomography. *Eurasian J Med* 2013; **45**:115–21.
10. Gibelli D, Cellina M, Cerutti S, Cattaneo C, Sforza C. Anatomical variations of anterior ethmoidal foramen and cribriform plate: relations with sex. *J Craniofac Surg* 2022; **33**:e2–4.
11. El-Taher M, Ahmed MA, Saleh HA, Ahmed YH. Coincidence of concha bullosa with nasal septal deviation: radiological study. *Indian J Otolaryngol Head Neck Surg* 2019; **71**:1918–22.
12. Stallman JS, Lobo JN, Som PM. The incidence of concha bullosa and its relationship to nasal septal deviation and paranasal sinus disease. *AJNR Am J Neuroradiol* 2004; **25**:1613–8.
13. Gun R, Ozcan I, Ozturk A, Yildiz A, Dogan M. The relationship between pneumatized middle turbinate and the anterior ethmoid roof dimensions: a radiologic study. *Eur Arch Otorhinolaryngol* 2013; **270**:1365–71.
14. Pérez P, Sabaté J, Carmona A, Catalina-Herrera CJ, Jiménez-Castellanos J. Anatomical variations in the human paranasal sinus region studied by CT. *J Anat* 2000; **197**:2217.
15. Hatipoglu HG, Cetin MA, Yuksel E. Nasal septal deviation and concha bullosa coexistence: CT evaluation. *B-ENT* 2008; **4**:227–32.
16. Kar M, Altintas M. The incidence of concha bullosa: a retrospective radiologic study. *Eur Arch Otorhinolaryngol* 2023; **280**:731–5.
17. El-Din WAN, Soliman NA, Mohamed SA, Abdelkhalek A, Elsayed AB. Prevalence of the anatomical variations of concha bullosa and its relation with sinusitis among Saudi population: a computed tomography scan study. *Anat Cell Biol* 2021; **54**:193–201.
18. Kalaiarasi R, Ramakrishnan V, Poyyamoli S. Anatomical variations of the middle turbinate concha bullosa and its relationship with chronic sinusitis: a prospective radiologic study. *Int Arch Otorhinolaryngol* 2018; **22**:368–73.
19. Cukurova I, Yaz A, Gumussoy M, Yigitbasi OG. A patient presenting with concha bullosa in another concha bullosa: a case report. *J Med Case Rep* 2012; **6**:87.
20. Güler C, Özkırış M, Kapsuz Z, Saydam L. Analysis of ethmoid roof and skull base with coronal section paranasal sinus computed tomography. *J Craniofac Surg* 2012; **23**:1460–4.
21. Uzun L, Savranlar A, Baskan Z, Aslan K, Aksoy F, Karasen RM. Is pneumatization of middle turbinates compensatory or congenital? *Dentomaxillofac Radiol* 2012; **41**:564–70.
22. Güldner C, Diogo I, Windfuhr JP, Bien S, Sesterhenn AM, Schick B. Potential of dosage reduction in cone-beam computed tomography for diagnostics of the paranasal sinuses. *Eur Arch Otorhinolaryngol* 2013; **270**:1307–15.
23. Acikalin RM, Ceylan M, Celik H, Karadag M. Is there a relationship between middle concha bullosa and ethmoid roof asymmetry? *Braz J Otorhinolaryngol* 2022; **88**:101–4.
24. De Cock J, Devriendt D, Demaerel P, Lemmerling M, Van Cauteren M, Hermans R. A comparative study for image quality and radiation dose of a cone-beam computed tomography scanner and a multislice computed tomography scanner for paranasal sinus imaging. *Eur Radiol* 2015; **25**:1891–900.
25. Dasar U, Gokce E. Evaluation of variations in sinonasal region with computed tomography. *World J Radiol* 2016; **8**:98–104.
26. Acikalin RM, Bayram O, Haci C, Yanik HT, Ozturkcu Y, Kocak A, Insan A. Is there a relationship between middle concha bullosa and ethmoid roof asymmetry? *Braz J Otorhinolaryngol* 2022; **88**:101–104.
27. Gun R, Yorgancilar E, Bakir S, Ekici F, Akkus Z, Ari

S, Topcu I. The relationship between pneumatized middle turbinate and the anterior ethmoid roof dimensions: a radiologic study. *Eur Arch Otorhinolaryngol* 2013; **270**:1365-71.

28. Kajan ZD, Sigaroudi AK, Ebrahimpour S. Effects of septal deviation, concha bullosa, and their combination on posterior palatal arch depth using cone-beam computed tomography. *J Dent Shiraz* 2016; **17**:26-32.

29. Roman RA, Neagoe RM, Roman SD, Popovici RE, Vlădan CI. Assessing prevalence of paranasal-sinus anatomical variants in patients with sinusitis using cone-beam computed tomography. *Clujul Med* 2016; **89**:423-9.

30. Damar M, Dinç AE, Eliçora SS, Bişkin S, Yıldırım M, Uslu S. Does the degree of septal deviation affect cribriform plate dimensions and middle turbinate length? *J Craniofac Surg* 2016; **27**:51-5.

31. Saylisoğlu S, Bayram M, Kantarci M, Calik M, Karazincir S, Alper F. Is there a relationship between cribriform plate dimensions and septal deviation angle? *Eur Arch Otorhinolaryngol* 2014; **271**:1067-71.